UNIVERSITÀ DEGLI STUDI DI PADOVA

Dipartimento di Fisica e Astronomia "Galileo Galilei"

Corso di Laurea in Fisica

Tesi di Laurea

Dust evolution in protoplanetary disks

Relatore

Prof. Francesco Marzari

Laureando

Annachiara Picco

Anno Accademico 2017/2018

Abstract

In this work we analysed some essential physics of a protoplanetary disk, then the most important models of dust dynamics are browsed, to conclude with a study of coagulative processes starting from the now classic Smoluchowski equation (1916), while following some more recent theoretical patterns and keeping an eye on order of magnitude estimates where possible.

Contents

Preface **v**

1 Protoplanetary Disks **1**
1.1 Stationary structure 2
1.2 Conservation laws and surface density evolution 4
1.3 Shakura-Sunyaev prescription 9

2 Dust evolution: generalities **13**
2.1 Aerodynamic relationships 13
2.2 Radial drift 15
2.3 Vertical settling 20

3 Coagulation **23**
3.1 Smoluchowski equation 24
3.2 Relative particles velocity 28
3.3 Differential settling and radial drift 32

Conclusions **37**

Preface

Disks are ubiquitous systems in astrophysics: protoplanetary disks, Debris disks, disk galaxies are examples of these flattened structures, varying by orders of magnitude in size and differing hugely in their composition, though sharing the same basic dynamics and many physical phenomena.
Accretion processes, i.e the extraction of gravitational potential energy from material which accretes on to a gravitating body, occur in most of them and make disks essential to stars, planets and satellites formation, rulers of super massive black holes growth too.

The past two decades have seen remarkable progress and profound, renewed interest in the study of protoplanetary disks, a kind of physical system whose speculation trace its roots in the eighteen century, with Pierre Simon de Laplace's model of the solar nebula (1756). This "nebular hypothesis" of a flattened, rotating structure as the origin of the observed coplanar planetary orbits was soon abandoned, yet pulling the trigger to a long history of theoretical interest, primarily regarding planets formation and accretion processes in protoplanetary disks. These topics were mature enough to accumulate a vast literature by the 1980s, when such disks were inferred from the infrared excesses of young stellar objects (hereafter YSO), then directly imaged in the sub-mm (Sargent and Beckwith, 1987 [2]; Koerner et al., 1993, [1]), and finally in the optical, with the examples in the Orion Nebula uncovered by the Hubble Space Telescope (McCaughrean and O'Dell, 1996, [3]).

Among the still developing research's branches, the theory of planet formation in protoplanetary disks, which tracks the agglomeration of solid particles from micron-sized dust to the 10^3 km cores of giant planets, is one of the key issue in modern astrophysics of today. This growth in the context of planets formation covers several orders of magnitude in spatial and mass scale and is dued to different physical processes, from self gravity and sticking collisions of small dust particles to core accretion of giant planets. Dust appears hence to be the protagonist of the the first stage of planets formation.

This work will browse the details of the early evolution of dusty protoplanetary disks surrounding YSO, with particular interest in the behavior of the dust. In particular the first chapter 1 will represents a brief (inevitably not comprehensive) overview of the general physics of protoplanetary disks with a classical model. Provided this necessary background, the second chapter 2 will discuss several general dust evolution processes, leading eventually to the third chapter 3, which will describe the coagulation paradigm through the well known Smoluchowski equation.

* * *

Chapter 1

Protoplanetary Disks

A protoplanetary disk is the result of the collapse of a molecular cloud of gas and dust due to gravity. Under the action of the competing forces associated with gravity, gas pressure, magnetic support and rotation, the contracting nebula begins to spin faster because of angular momentum conservation, as it starts to flatten, under the effect of stronger centrifugal forces, into a spinning disk with a bulge at the center. The instabilities in the collapsing and rotating cloud cause localized gravitational collapses, and the bulge becomes the central star.

Eventually the disk is composed by relatively cool primarily molecular gas, mostly H_2, scattered with dust. Table 1.1 shows some typical parameters and the relative orders of magnitude, with $H_p(r)$ as the density scale-height. The dust represents a trace population of solids, with an average dust-to-gas ratio $f \sim 0.01$ similarly to the solar value.

Parameters	Values
Masses M	$10^{-3} M_\odot$ to $10^{-1} M_\odot$
Sizes	100 AU to 1000 AU
Lifetimes	10^6 yr to 10^7 yr
Temperature	100 K to 1000 K
Thickness H_p/r	0.03 to 0.05
Number density n	$10^9\,\mathrm{cm}^{-3}$ to $10^{18}\,\mathrm{cm}^{-3}$

Table 1.1: Characteristic scales for some parameters of interest (estimates lifted from [4], [5], [6]).

In the following sections we will discuss the most important theoretical concepts of circumstellar disk's surrounding gas, treating gaseous medium as a continuous fluid, by virtue of such value of f, with a z-axissymmetric flow around the central gravitating star of mass M_*. We also assume the fluid to

be unmagnetised, for a magnetohydrodynamic (MHD) rigorous theorisation would be far beyond the scope of this work.

1.1 Stationary structure

Let us start with the equation of motion for an inviscid, unmagnetised gaseous fluid with pressure $P(r,z,t)$, density $\rho_g(r,z,t)$, surface density $\Sigma_g(r,z,t)$ and velocity field $\mathbf{u_g}(r,z,t)$. We adopt cylindrical polar coordinates (r,ϕ,z) such that the central mass is at $r=0=z$ and the mid-plane of the disk is $z=0$. The so called Euler equation is:

$$\frac{D\mathbf{u_g}}{Dt} = \frac{\partial \mathbf{u_g}}{\partial t} + (\mathbf{u_g}\cdot\nabla)\,\mathbf{u_g} = -\frac{1}{\rho_g}\nabla P - \nabla\Phi, \tag{1.1}$$

where D/Dt is the Lagrangian time-derivative following the fluid flow and Φ is the gravitational potental.

i) *Vertical structure*

Solving the Eq. (1.1) for hydrostatic equilibrium combined with the Poisson equation for the gravitational potential is nontrivial (Papaloizou and Pringle, 1984) [7]. For a straightforward resolution at a given time we assume $M_{disk} \ll M_*$, so that $\Phi = \Phi(r,z)$ is dominated by stellar gravity. Then the z-component for hydrostatic equilibrium of Eq. (1.1) is:

$$\frac{1}{\rho_g}\frac{\partial P}{\partial z} = \frac{\partial}{\partial z}\left(\frac{GM_*}{(r^2+z^2)^{1/2}}\right). \tag{1.2}$$

Assuming also a vertically isothermal structure with constant sound speed c_s and pressure $P=\rho_g c_s^2$, Eq. (1.2) becomes

$$c_s^2\frac{1}{\rho_g}\frac{\partial \rho_g}{\partial z} = -\frac{GM_* z}{(r^2+z^2)^{3/2}},$$

which integrates to give

$$\rho_g(r,z) = \rho_0\ \exp\left\{r^2\frac{\Omega_K^2}{c_s^2}\left[\left(1+\frac{z^2}{r^2}\right)^{-1/2} - 1\right]\right\}.$$

Here $\Omega_K = \sqrt{GM_*/r^3}$ is the Keplerian orbital velocity at distance r on the midplane and the isothermal sound speed is as usual defined $c_s^2 = k_B T/\mu m_p$ where μ is the mean molecular weight in units of the proton mass m_p. The density shows negligibly small departures from a gaussian profile centered on the mid-plane, and with the thin disk assumption such that $z \ll r$, and $H_p(r)/r \ll 1$ invariably in the disk, we obtain an exact Gauss' distribution

$$\rho_g(z) = \rho_0 e^{-z^2/2H_p^2}, \tag{1.3}$$

where we have the vertical scale height H_p given by $H_p \equiv c_s/\Omega_K$, and the mid-plane density ρ_0 is related to the surface density

$$\Sigma_g = \frac{1}{2\pi}\int_0^{2\pi}\int_{-\infty}^{\infty}\rho_g(z)\,dz\,d\phi \tag{1.4}$$

by the normalisation condition

$$\Sigma_g = \sqrt{2}H_p\rho_0\int_{-\infty}^{\infty}e^{-z^2/2H_p^2}\,d\left(z/\sqrt{2}H_p\right) \quad \Rightarrow \quad \rho_0 = \frac{1}{\sqrt{2\pi}}\frac{\Sigma_g}{H_p}.$$

Detailed disk models show that disks actually are geometrically thin, with $H_p/r \approx 0.05$ being fairly typical as showed in Tab. (1.1) (e.g. Bell et al., 1997, [8]), which makes our assumption justified. As regards the validity of the assumption of a negligible contribution of the disk itself to the vertical component of gravity, we shall give a rough estimate representing the disk as an infinte sheet of mass with the surface density Σ_g. Gauss' theorem shows that gravitational acceleration g_z above the sheet is independent of height, $g_z = 2\pi G\Sigma_g$. Comparing this acceleration with the vertical component of the star's gravity at $z = H_p$ allows us to give a condition for the disk's own gravity to be negligible:

$$\Sigma_g < \frac{M_*}{2\pi}\frac{H_p}{r^3} \quad \Rightarrow \quad \frac{M_{disk}}{M_*} \lesssim \frac{H_p}{r}, \tag{1.5}$$

where we have very roughly written $M_{disk} \sim \pi r^2\Sigma_g$. We shall see that, for $H_p(r)/r \approx 0.05$, a disk mass of a few percent of M_* makes a non negligible change to the vertical structure.

ii) *Radial structure*

Let us now investigate the azimuthal velocity in the mid-plane $u_{\phi,g} = u_{\phi,g}(r)$ of the gas. The radial component of the Euler equation Eq. (1.1) for the considered stationary axissymmetric gaseous flow at $z = 0$ is given by

$$\frac{u_{\phi,g}^2}{r} = \frac{GM_*}{r^2} + \frac{1}{\rho_g}\frac{\partial P}{\partial r}. \tag{1.6}$$

Since the gas pressure in disks generally decreases with increasing radius near the mid-plane, the pressure gradient provides an additional outward force, and the gas orbits at slightly sub-Keplerian speeds. If we approximate the gas pressure at the mid-plane as a power-law $P \propto r^{-n}$, and adopt a locally isothermal equation of state $P = \rho_g c_s^2$, then the pressure gradient term in Eq. (1.6) becomes

$$\frac{1}{\rho_g}\frac{\partial P}{\partial r} = -n\frac{c_s^2}{r}.$$

Substituting for this term in Eq. (1.6) we obtain

$$u_{\phi,g}^2 = u_K^2\left(1 - n\frac{c_s^2}{u_K^2}\right) = u_K^2\left(1-\eta\right), \tag{1.7}$$

in which the parameter η denotes how much the gas azimuthal velocity departs from Keplerian speed, and the power index n depends on the disk's radial density and temperature profiles. Let us stress that, recalling H_p definition, such deviations are $\mathcal{O}\left((H_p/r)^2\right)$, and hence small in the thin disk approximation.

We shall underline that the approximation of the thin disk is such that, in the mid-plane,

$$H_p = c_s \left(\frac{R}{GM_*}\right)^{1/2} R \ll R \quad \Leftrightarrow \quad c_s \ll \left(\frac{GM_*}{R}\right)^{1/2},$$

hence, for a thin disk, the local Kepler velocity is required to be highly supersonic.

1.2 Conservation laws and surface density evolution

The accretion mechanism is qualitatively described by the extraction of gravitational potential energy from disk's population, which accretes to the central star, combined with the outward redistribution of specific angular momentum $h(r)$. The phenomena responsible for this process remain unclear: following here a classical approach, we trace the evolution of an axissymmetric, geometrically thin protoplanetary disk in which dissipation leading to accretion is formally due to molecular viscosity ν. In section 1.3 we shall give a brief discussion on the limits of this description.

We will start from the mass conservation law combined with Navier-Stokes equation of motion for the viscous gaseous fluid with the usual coordinates (r, ϕ, z):

$$\frac{\partial \rho_g}{\partial t} + \nabla \cdot (\rho_g \mathbf{u_g}) = 0, \tag{1.8}$$

$$\frac{D\mathbf{u_g}}{Dt} = -\frac{1}{\rho_g}\nabla P - \nabla\Phi + \frac{1}{\rho_g}\nabla \cdot \mathbf{T}, \tag{1.9}$$

where $\mathbf{T}$ is the stress tensor, a symmetric tensor field of second rank.

i) *Mass conservation*

Let us specialize the mass conservation law to our case, taking into account the hypothesis of an axissymmetric flow and the thin disk approximation. Eq. (1.8) then reads

$$\frac{\partial \rho_g}{\partial t} + \frac{1}{r}\frac{\partial}{\partial r}\left(r\rho_g u_{r,g}\right) + \frac{1}{r}\frac{\partial}{\partial \phi}\left(\rho_g u_{\phi,g}\right) + \frac{\partial}{\partial z}\left(\rho_g u_{z,g}\right) = 0, \tag{1.10}$$

where the components of the gas velocity are plainly indexed and the last two left-hand side terms are hence zero. Recalling definition 1.4, Eq.

(1.10) integrates with respect to ϕ and z over the full extent of the disk to give

$$\frac{\partial \Sigma_g}{\partial t} + \frac{1}{r}\frac{\partial}{\partial r}\left(r\Sigma_g \bar{u}_r\right) = 0, \tag{1.11}$$

in which we introduced a (density-weighted) mean radial velocity $\bar{u}_r$, whose definition is given in terms of another useful quantity, the flux $\mathcal{F}(r,t)$, as follows

$$\mathcal{F}(r,t) = 2\pi r \bar{u}_r \Sigma_g = \int_0^{2\pi}\int_{-\infty}^{\infty} r\rho_g u_r \, dz \, d\phi. \tag{1.12}$$

We shall eventually give another form of the mass conservation law, Eq. (1.11), which will be employed later.

$$\frac{1}{2\pi}\frac{\partial \Sigma}{\partial t} + \frac{1}{r}\frac{\partial \mathcal{F}}{\partial r} = 0 \tag{1.13}$$

ii) *Specific angular momentum conservation*

We will now specialize Eq. (1.9) as well, writing its azimuthal component as follows:

$$\rho_g\left(\frac{D}{Dt}\left(ru_{\phi,g}\right) + \frac{u_{\phi,g}u_{r,g}}{r}\right) = -\frac{\rho_g}{r}\frac{\partial \Phi}{\partial \phi} - \frac{1}{r}\frac{\partial P}{\partial \phi} + \\ + \frac{1}{r^2}\frac{\partial}{\partial r}\left(r^2 T_{r\phi}\right) + \frac{1}{r}\frac{\partial T_{\phi\phi}}{\partial \phi} + \frac{\partial T_{\phi z}}{\partial z}, \tag{1.14}$$

in which the diagonal components of the stress tensor $\mathbf{T}$ are plainly indexed. In our axissymmetric system the first two right-hand side terms are zero and the azimuthal velocity u_ϕ in the disk is given by $u_\phi = r\Omega(r)$, taking into account the small deviations from a Keplerian rotation curve (Eq. (1.7)) and assuming a circular orbit motion with angular velocity Ω. The specific angular momentum $h(r)$ is then given by

$$h(r) = ru_{\phi,g} = r^2\,\Omega(r). \tag{1.15}$$

In this circular orbital motion, in particular, the only stress tensor component is

$$T_{\phi r} = T_{r\phi} = \nu\rho_g r\frac{\partial \Omega}{\partial r},$$

i.e. the viscosity multiplied by the shear rate. Then Eq. (1.14) develops as follows

$$\rho_g \frac{D}{Dt}\left(u_{\phi,g} r\right) = \frac{1}{r}\frac{\partial}{\partial r}\left(r^2 T_{r\phi}\right) \quad \Leftrightarrow \quad \rho_g u_{r,g}\frac{dh}{dr} = \frac{1}{r}\frac{\partial}{\partial r}\left(\rho_g \nu r^3 \frac{d\Omega}{dr}\right),$$

and, multiplying by r, the integration with respect to ϕ and z finally leads to

$$\Sigma_g \bar{u}_r \frac{dh}{dr} = \frac{1}{r}\frac{\partial}{\partial r}\left(\bar{\nu}\Sigma_g r^3 \frac{d\Omega}{dr}\right). \tag{1.16}$$

We introduced a (density-weighted) mean kinematic viscosity $\bar{\nu}(r,t)$, whose definition is given in terms of another useful quantity, the torque $\mathcal{G}(r,t)$, as follows

$$\mathcal{G}(r,t) = -\int_0^{2\pi}\int_{-\infty}^{\infty} r^2 T_{r\phi}\, dz\, d\phi = -2\pi r \cdot \bar{\nu}\Sigma_g r \frac{d\Omega}{dr} \cdot r \tag{1.17}$$

The quantity $\mathcal{G}$ has the physical meaning of the torque acting on an annulus in our gaseous disk at the radial coordinate r, and it is the product of the circumference, the viscous force per unit lenght and the lever arm r, being proportional to the gradient of the angular velocity too. We shall give another form of the momentum conservation law Eq. (1.16) as well, which will be employed later.

$$\mathcal{F}\frac{dh}{dr} + \frac{\partial \mathcal{G}}{\partial r} = 0. \tag{1.18}$$

We can now use these ruling conservation laws to investigate the surface density $\Sigma_g(r,t)$ evolution. Equations (1.11) and Eq. (1.16) may be combined to eliminate $\bar{u}_r$, leading after some calculations to

$$\frac{\partial \Sigma_g}{\partial t} + \frac{1}{r}\frac{\partial}{\partial r}\left[\left(\frac{dh}{dr}\right)^{-1}\frac{\partial}{\partial r}\left(\bar{\nu}\Sigma_g r^3 \frac{d\Omega}{dr}\right)\right] = 0$$

$$\Leftrightarrow \quad \frac{\partial \Sigma_g}{\partial t} = \frac{3}{r}\frac{\partial}{\partial r}\left[r^{1/2}\frac{\partial}{\partial r}\left(r^{1/2}\bar{\nu}\Sigma_g\right)\right],$$

which has the character of a diffusion equation for the surface density, to be interpreted as the diffusion effect due to viscous torque affecting $\Sigma_g(r,t)$ and causing it to spread in time. For this last passage we have taken $\Omega(r) = \Omega_K$.

The diffusion equation for the surface density hence incorporates the meaning of the accretion process, yet being harsh to treat analitically, apart from assuming simple forms of the viscosity $\bar{\nu}$ (hereafter simply ν for clarity). Here we follow the now-classic paper from Lynden-Bell & Pringle (1974) [9] in deriving an interesting solution with Green's function method for a constant ν, with the boundary conditions of zero torque at $r = 0$. Substituting Eq. (1.18) and Σ_g obtained from Eq. (1.17) in Eq. (1.13), we find

$$\frac{\partial}{\partial t}\left[\frac{\mathcal{G}}{r^2\nu\frac{d\Omega}{dr}\frac{dh}{dr}}\right] - \frac{\partial^2 \mathcal{G}}{\partial h^2} = 0, \tag{1.19}$$

which has the character of a diffusion equation as well, describing the torque diffusing in the space of specific angular momentum. If we remember now that in our case $\Omega(r) = \Omega_K$ and $h(r) = (GM_* r)^{1/2}$, we can easily rewrite the denominator of the right-hand side term as

$$r^2\nu\frac{d\Omega}{dr}\frac{dh}{dr} = \frac{1}{4}\gamma^{-2}h^{-2}\,,$$

where we imposed $\gamma^{-2} = 3\nu(GM_*)^{1/2}$ for future simplicity. Then Eq. (1.19) reads

$$\frac{\partial^2 \mathcal{G}}{\partial h^2} = 4\gamma^2 h^2 \frac{\partial \mathcal{G}}{\partial t}.$$

Let us now assume that $\mathcal{G} \propto e^{-st}$ where s is a parameter. Defining $k^2 = s\gamma^2$, we obtain

$$\frac{\partial^2 \mathcal{G}}{\partial h^2} + 4kh^2\mathcal{G} = 0, \tag{1.20}$$

and by means of the following transformations

$$x = h^2, \quad \frac{\partial^2}{\partial h^2} = 2x^{1/2}\frac{\partial}{\partial x}\left(2x^{1/2}\frac{\partial}{\partial x}\right), \quad \mathcal{G}' = x^{-1/4}\mathcal{G},$$

Eq (1.20) is reconducible to a Bessel differential equation of order 1/4:

$$\frac{\partial^2 \mathcal{G}'}{\partial x^2} + \frac{1}{x}\frac{\partial \mathcal{G}'}{\partial x} + \left(k^2 - \frac{1}{4^2x^2}\right)\mathcal{G}' = 0\ . \tag{1.21}$$

This equation has the following well known elementary solutions (hereafter we rename $\mathcal{G}' \to \mathcal{G}$ for simplicity)

$$\mathcal{G}(x,t) = e^{-st}(kx)^{1/4}\left[A(k)J_{1/4}(kx) + B(k)J_{-1/4}(kx)\right]$$

where $J_{\pm 1/4}(kx)$ are the Bessel functions of order $\pm 1/4$ and $A(k)$, $B(k)$ are the modes coefficients. Imposing the boundary condition on torque, i.e. that $\mathcal{G}(0,t) = 0$, we straightforwardly get that $B(k) = 0$. So the general solution of Eq. (1.21) is given by the following integration on modes:

$$\mathcal{G}(x,t) = \int_0^\infty dk\, e^{-st}(kx)^{1/4}\left[A(k)J_{1/4}(kx)\right]. \tag{1.22}$$

Interpreting this solution as the Hankel transform

[1]

of $A(k)$, we get that, antitrasforming,

$$A(k) = \int_0^\infty dx\,(kx)^{3/4}J_{1/4}(kx)\mathcal{G}(x,0). \tag{1.24}$$

As previously stated, we can study the properties of Eq.(1.21) solution by Green's functions, observing that it can be thought of as made up of elementary

[1]The Hankel transform of order ν of a function $f(x)$ is defined as:

$$F_\nu(k) = \int_0^\infty f(x)J_\nu(kx)x\,dx, \tag{1.23}$$

where J_ν is the Bessel function of the first kind of order ν with $\nu \geq -1/2$. The inverse Hankel transform of $F_\nu(k)$ is defined as:

$$f(x) = \int_0^\infty F_\nu(k)J_\nu(kx)k\,dk.$$

solutions whose initial density distribution are characterized by the following form

$$\Sigma_g\left(r, t=0\right) = \frac{m}{2\pi r_0}\delta\left(r - r_0\right),$$

where the $\delta\left(r - r_0\right)$ is a Dirac delta function with the physical meaning of a peaked initial distribution of the thin gas ring of mass m at radius r_0. The correspondent torque $\mathcal{G}\left(x, 0\right)$ to the initial Σ_g is hence

$$\mathcal{G}\left(x, 0\right) = \frac{1}{4}\gamma^{-2}h_1^{-2}\delta\left(h - h_0\right) = \frac{1}{2}m\gamma^{-2}x^{-1/2}\delta\left(x - x_0\right),$$

where we used the torque definition (1.17) and performed a coordinates changing from (r, r_0) to (h, h_0) and finally to (x, x_0). The mode coefficient $A(k)$ is now known from Eq. (1.24) , which directly leads to

$$A(k) = \frac{1}{2}m\gamma^{-2}x_0^{1/4}k^{3/4}J_{1/4}\left(kx_0\right),$$

and the torque $\mathcal{G}(x, t)$ comes from Eq. (1.22):

$$\mathcal{G}(x, t) = \frac{1}{2}\gamma^{-2}mx_0^{1/4}x^{1/4}\int_0^\infty dke^{-\frac{k^2t}{\gamma^2}}kJ_{1/4}\left(kx_0\right)J_{1/4}\left(kx\right).$$

This integral may be found in the Tables of Hankel transforms, yielding

$$\mathcal{G}(x, t) = \frac{m}{2}\gamma^{-2}\frac{\left(x_0x\right)^{1/4}}{x_0^2\,T_*}\exp\left[-\left(\frac{x_0^2 + x^2}{4\gamma^{-2}t}\right)\right]I_{1/4}\left(\frac{xx_0}{2\gamma^{-2}t}\right), \tag{1.25}$$

where $T_* = 2\gamma^{-2}t/x_0^2$, and $I_{1/4}(z)$ is the modified Bessel function of order $1/4$. Finally we can write the solution for $\Sigma_g(r, t)$ from this solution for the torque, using the definition in Eq. (1.17) and the dimensionless variables $\mathcal{X} = r/r_0$ and $\tau = 12\nu r_0^{-2}t$.

$$\Sigma_g(\mathcal{X}, \tau) = \frac{m}{\pi r_0^2}\frac{1}{\tau}\mathcal{X}^{-1/4}\exp\left[-\frac{\left(1 + \mathcal{X}^2\right)}{\tau}\right]I_{1/4}\left(\frac{2\mathcal{X}}{\tau}\right). \tag{1.26}$$

The time-dependent solution for $\mathcal{G}(x, t)$ and $\Sigma_g(\mathcal{X}, \tau)$ for arbitrary initial conditions can be formally written as a superposition of the solutions found in Eq. (1.25) and Eq. (1.26). We plotted in Fig.(1.1) the $\Sigma_g(\mathcal{X}, \tau)$ profile as function of the scaled time variable for some values of τ.

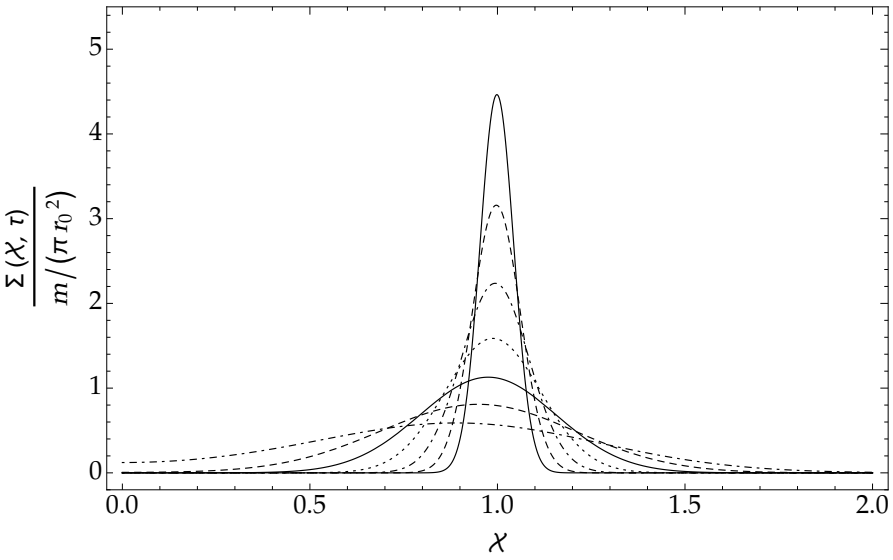

Figure 1.1: The time-dependent solution $\Sigma_g(\mathcal{X},\tau)$ in units of $m/(\pi r_0^2)$ as a function of the scaled time variable τ, showing the spreading of Σ_g for a ring of gas initially orbiting at $r = r_0$ (hence $\mathcal{X} = 1$). From top down (solid, dashed, dotdashed, dotted) the curves are about $\tau = 0.004$, $\tau = 0.008$, $\tau = 0.016$, $\tau = 0.032$, $\tau = 0.064$, $\tau = 0.128$, $\tau = 0.256$.

1.3 Shakura-Sunyaev prescription

We will now briefly browse the limits of our previous classical description. We stress that until now we have assumed a cinematic viscosity ν to be responsible for the redistribution of angular momentum toward the outskirts of the disk. Viscous stresses between annuli of gaseous parcels, besides, appear to be the most logical and intuitive hypotetical key-process. By setting $\left(1+\mathcal{X}^2\right)\tau^{-1} \sim \mathcal{X}^2\tau^{-1} \sim 1$ in the argument of the exponential in Eq. (1.26), we shall define the viscous time-scale τ_ν, for a disk with characteristic size r, as follows

$$\tau_\nu \equiv \frac{r^2}{\nu}, \tag{1.27}$$

with the physical meaning of the amount of time required for viscous accretion to alter the surface density (locally). Trying to make an estimate, we can define two characteristic physical quantities for the system, the mean thermal velocity $\bar{u}$ and the mean free path $\lambda_{\rm mfp}$ between the gas molecules

$$\bar{u} = \left(\frac{8k_BT}{\pi\mu m_p}\right)^{1/2} = \left(\frac{8}{\pi}\right)^{1/2} c_s, \qquad \lambda_{\rm mfp} = \frac{\bar{u}}{\mathcal{N}} = \frac{1}{n\sigma}, \tag{1.28}$$

in which the mid-plane number of molecules per unit volume equals n, $\sigma \sim \sigma_{H_2}$ is the collision cross-section (the gas molecules are assumed to be mainly diatomic hydrogen) and the number of collisions per second experienced by a given molecule is calculated as $\mathcal{N} = n\pi b^2(8k_BT/\pi\mu m_p)$, b being a molecular radius; $\bar{u}$ is a well known thermodynamic result easily derivable from

the Maxwellian probability distribution for the molecular speed. To order of magnitude precision, the viscosity of a gaseous system may be written as $\nu \sim \lambda_{\mathrm{mfp}} \bar{u}$ and, taking into account appropriate conditions at 1 AU (i.e. $\sigma_{H_2} = 2 \times 10^{-15}\,\mathrm{cm}^2$ lifted from [10], $n = 10^{15}\,\mathrm{cm}^{-3}$, $\bar{u} = 10^5\,\mathrm{cm\,s}^{-1}$), we find

$$\nu \sim 5 \times 10^4\,\mathrm{cm}^2\,\mathrm{s}^{-1},$$

which, using the definition of viscous time-scale Eq. (1.27), reads

$$\tau_\nu \sim 10^{13}\,\mathrm{yr},$$

i.e. a time-scale of several orders of magnitude longer than the lifetime typically assigned to the protoplanetary disks, keeping in mind Tab. (1.1). Molecular viscosity is hence too small to account for the observed mass accretion rates. The description provided in the previous section is, however, approximately valid if the cinematic viscosity considered above is re-interpreted as the outcome of a turbulent process. The incredibly high values of the fluid Reynolds number $Re_g \sim H_p c_s/\nu$ (taken e.g. $c_s = 0.5\,\mathrm{km\,s}^{-1}$ at 10 AU and $H_p = 0.05r$) seem to favor this hypothesis: it is reasonable to think Re_g for the gas to be far beyond the critical Reynolds number Re_c at which turbulence sets in (Re_c is observed to be consistently lower by terrestrial standards (Eckhardt et al., 2007, [11]).

Inspired by this fact Shakura and Sunyaev (1973) [12] parameterized, using merely dimensional argumentations, the unknown turbulent viscosity as the product of a velocity scale and a lenght scale, for which the largest reasonable values are indeed H_p and c_s, both evaluated at the disk mid-plane. We follow their work writing

$$\nu = \alpha c_s H_p, \tag{1.29}$$

where α, obviously expected to be $\alpha \lesssim 1$, is the famous dimensionless parameter which takes its name from Shakura & Sunyaev and account for the efficiency of angular momentum transport due to turbulence. This prescription has hence the virtue to satisfy dimensional considerations and to be extremely simple, however as for the numerical value of the parameter there is little known. Often, α is taken to be constant with a value $10^{-3} < \alpha < 10^{-2}$ (Johansen & Klahr, 2005; Dzyurkevich et al., 2010 [13], [14]), but we stress the lack of physical hints justifying this assumption. Giving another order of magnitude estimate, using $\alpha = 10^{-3}$ and appropriate conditions at 1 AU ($H_p = 0.05r$ and $c_s \sim 10^5\,\mathrm{cm\,s}^{-1}$) we find

$$\nu = 7.5 \times 10^{13}\,\mathrm{cm\,s}^{-1},$$

which, using the definition of viscous time-scale in Eq. (1.27), yields to

$$\tau_\nu \sim 10^4\,\mathrm{yr}.$$

This viscosity is circa eight orders of magnitude larger than the molecular viscosity calculated before, and now there is good agreement with the observed

disks' lifetimes. The question about the origin of the postulated turbulence is still open, taking into account that the so called Railegh criterion (a slightly lenghty derivation is due to Pringle & King, 2007 [15]) prevent a Keplerian rotating flow to be unstable to infinitesimal hydrodynamic perturbations, in absence of magnetic fields and in low-mass condition (Eq. (1.5)). The magnetorotational instability (hereafter MRI), present in weakly magnetized disks, is the most accepted mechanism to drive turbulence in disks (Balbus and Hawley, 1991 [16]), being expected to sustain a dynamically significant magnetic field and to provide measurable angular momentum transport. Theories propose that angular momentum can also be transferred by global processes like gravitational instabilities (GI).

A comprehensive treatment of this problem would be far beyond our scopes, anyway a general overview on some now-classic (and modern as well) theories was needed, since it should be evident that each phenomenon underlying the transport of angular momentum may be more or less decisive in the evolution of the dust, which is the subject of the following chapter.

* * *

Chapter 2

Dust evolution: generalities

Planets form from dust in protoplanetary disks and growth in size by many orders of magnitude is involved, with different mechanisms operating in various size regimes. By terms of the usual nomenclature, we refer as *dust* to material grains from the sub-micron size to centimeter size, to meter size bodies as *rocks*, to 10 km size masses as *planetesimals*. From the scale of 1000 km on, then, as actual *planets*. The formation mechanism of rocks and small agglomerate of dust involves sticky collisions due to molecular forces, while the formation of (giant) planets resolves around merging due to gravitational attraction and accretion.

In the previous section we have briefly described the initial infall phase of a molecular cloud shaping a protoplanetary disk. As we know, as the flattening nebula radiates energy and gradually cooled, different elements and compounds start to condense and form solid dust grains, with the evidence that whether a substance exists as a solid or a gas depends on the condensation sequence, which is dependent on the local pressure and temperature of the nebula itself: refractory materials (stable at relatively high temperatures) as well as volatile materials can be accounted in different regions of the disk.

In the following sections our attention will be focused in the early stages of planets formation, studying the dust dynamics with classical equations of motions, keeping an eye on order of magnitude estimates where possible. In particular we shall describe in details the effect of the gaseous medium on the dust dynamics, yet implicitly assuming the reciprocal effect to be negligible by virtue of the small value of the dust-to-gas ratio $f \sim 0.01$, which is only partially true. Anyway we shall not deepen the issue.

2.1 Aerodynamic relationships

Solid bodies are unaffected by pressure gradients, yet experiencing forces exerted by the gaseous medium in which are sommersed, due to the relative

velocity Δu with respect to the fluid. These forces are summed up in the process of aerodynamic drag, and in this section we will describe its various forms and different regimes which determine the dust-to-gas coupling.

Consider a solid particle of mass m, that we assume to be spherical with radius a and solid density ρ_s, moving through a gas of (local) density ρ_g at velocity Δu. The mean free path of the gas molecules is $\lambda_{\rm mfp}$ and the gas is characterized by the thermal velocity $\bar{u}$ as defined above, Eq. (1.28). Which aerodynamic regime applies to a certain particle depends on the ratio between $\lambda_{\rm mfp}$ and a, i.e. the Knudsen number K_n, such that the drag force $\mathbf{F_D}$ in a neutral gas can be written as follows

$$\mathbf{F_D} = \frac{1}{2} C_D \pi a^2 \rho_g \Delta \mathbf{u}^2 \qquad \text{in the fluid regime with } K_n \lesssim 1, \tag{2.1}$$

$$\mathbf{F_D} \simeq \frac{4}{3} \pi \rho_g a^2 \bar{u} \Delta \mathbf{u} \qquad \text{in the particle regime with } K_n \gtrsim 1, \tag{2.2}$$

where the dimensionless drag coefficient C_D is related to the particle's geometry, in general a function of its Reynolds number Re, which can be written:

$$Re = \frac{2a\Delta u}{\nu_{\rm mol}}, \qquad \nu_{\rm mol} = \frac{1}{2}\bar{u}\lambda_{\rm mfp}, \tag{2.3}$$

with $\nu_{\rm mol}$ being the molecular viscosity of the gas. It should be noted that Eq. (2.2), the so called Epstein regime, is simply (volume swept per unit time) $\times$ (momentum per unit volume). The conditions expressed in Eq. (2.1) and Eq. (2.2) can be interpreted as follows: $K_n \simeq 1$ marks the limit between the case in which $a \lesssim \lambda_{\rm mfp}$, i.e. the gas on the scale of the particle is effectively a collisionless ensemble of molecules with a Maxwellian velocity distribution, and the Stokes regime where $a \gtrsim \lambda_{\rm mfp}$, i.e. the gas flows around the obstruction of the particles.
The drag coefficient of a sphere, in the case of $Re < 1$, can be written taking into account the well known Stokes law $|F_D| = 6\pi\rho_g\nu_{\rm mol}a\Delta u$, i.e. $C_D = 24\, Re^{-1}$, being slightly more complicated for higher values of Re (Whipple, 1972 [17] and Weidenschilling, 1977 [18]). The Stokes and Epstein drag forces are evidently equal when $\lambda_{\rm mfp}/a = 4/9$; this is taken to be the transition point between the two laws.

Let us now define a key-parameter for the description of the aerodynamic coupling which simplifies the various forms of the drag equation, the *stopping time* t_s, and the dimensionless stopping time τ_s, also called the *Stokes number* St, as follows

$$t_s \equiv \frac{m\Delta u}{|F_D|}, \qquad \tau_s \equiv t_s \Omega_K, \tag{2.4}$$

with the physical meaning of the time needed from the drag force to modify the relative velocity significantly, and the level of relation between t_s and the orbital time at the location of the particle. For the drag laws of Eq. (2.1) and Eq. (2.2) we then find

$$t_s = \frac{2\rho_s a^2}{9\nu_{\rm mol}\rho_g} \qquad \text{Stokes regime with } \lambda_{\rm mfp}/a \lesssim 4/9 \text{ and } Re < 1, \tag{2.5}$$

$$t_s = \frac{\rho_s a}{\rho_g \bar{u}} = \frac{3}{4}\frac{m}{\sigma}\frac{1}{\rho_g \bar{u}} \qquad \text{Epstein regime with } \lambda_{\rm mfp}/a \gtrsim 4/9, \tag{2.6}$$

where we have written the particle mass as $m = 4/3\pi a^3 \rho_s$ and the factor m/σ is the mass-to-crosssection ratio. It is worth noticing that t_s, for Epstein drag, is a function of the particle properties, independent of Δu. Let us write another useful order of magnitude estimate: giving appropriate values at the mid-plane of a protoplanetary disk at 1 AU ($\rho_g = 10^{-9}\,\mathrm{g\,cm^{-3}}$, $\rho_s = 3\,\mathrm{g\,cm^{-3}}$, $\bar{u} = 10^5\,\mathrm{cm\,s^{-1}}$), for a particle of size $a = 1\,\mu$m, we obtain

$$t_s \approx 3\,\mathrm{s},$$

which allows us to conclude that small dust particles are very tightly coupled to the gas. The mean free path in protoplanetary disks is generally of the order of *cm* (for a typical nebula value $\lambda_{\rm mfp} \sim 1$ cm), so the Epstein regime is predominantly relevant for particles that range from dust grains to those of small macroscopic dimensions.
It is interesting to observe that in either regime, recalling Eq. (2.1) and Eq. (2.2), the drag force scales with the frontal area πa^2 that the particle presents to the gas, becoming hence negligible for macroscopically large bodies.

2.2 Radial drift

In section 1.1 we have seen that the radial pressure gradients result in a gas orbital velocity that differs from the Keplerian value u_K, in particular when the mid-plane pressure can be locally written as a power-law in radius such difference is $\mathcal{O}((H_p/r)^2)$, yet non negligible in absolute terms. This velocity deviation actually affects the evolution of solid particles in various limits, defined by the asymptotic behavior of τ_s:

i) $\tau_s \ll 1$: small dust particles are affected by a large drag force F_D and are strongly coupled to the gas, so that the grain would be stopped in a time t_s which is a small fraction of the orbital one;

ii) $\tau_s \gg 1$: dust or planetesimals are weakly affected by aerodynamic forces, which can be regarded as perturbations to the body's orbital motion, such that they would not be stopped for time comparable to or greater than the period of revolution.

We will now derive the rate of radial drift of the particles, without assumptions about τ_s, keeping for later a discussion about the above descripted limits. The equations of motion of the spherical grain are the following

$$\frac{du_{r,d}}{dt} = \frac{u_{\phi,d}^2}{r} - \Omega_K^2 r - \frac{1}{t_s}\left(u_{r,d} - u_{r,g}\right), \tag{2.7}$$

$$\frac{d}{dt}\left(r u_{\phi,d}\right) = -\frac{r}{t_s}\left(u_{\phi,d} - u_{\phi,g}\right), \tag{2.8}$$

with the subscripts clearly distinguishing gas and dust and Eq. (2.8) being the equality between the rate of change of angular momentum and the drag torque in terms of the stopping time. In Eq. (2.7) the first term is the centrifugal acceleration, the second term the acceleration due to gravity, and the third term the frictional drag force. We follow Takeuchi & Lin (2002), [19], since we do not solve the equation of motion in the z-direction. We are simply assuming a vertical equilibrium in which the dust sedimentation to the mid-plane is balanced by the diffusion of particles, as we will see in the end of this section. The vertical velocity $u_{z,d}$ of a particle is hence zero when time averaged.
We now make the simplifying assumption that the particles follow nearly circular orbits, i.e. $u_{r,d} \ll u_{\phi.d}$, such that motions of both the gas and the particles are close to Keplerian:

$$u_{\phi,d} \simeq u_{\phi,g} \simeq u_K, \qquad \frac{d}{dt}\left(r u_{\phi,d}\right) \simeq u_{r,d}\frac{d}{dr}(r u_K) = \frac{1}{2} u_{r,d} u_K,$$

which allows us to simplify the azimuthal equation Eq. (2.8), yielding

$$(u_{\phi,d} - u_{\phi,g}) \simeq -\frac{1}{2}\frac{t_s u_{r,d} u_K}{r}. \tag{2.9}$$

The next assumption we make is that the net acceleration in the radial direction $du_{r,d}/dt$ is negligible [1], which allows us to set the lef-hand side of Eq. (2.7) to zero. Substituting for Ω_K in the radial equation using Eq. (1.7) such that

$$\Omega_K^2 r = \frac{u_{\phi,g}^2}{r} + \eta\frac{u_K^2}{r}, \qquad (u_{\phi,d} + u_{\phi,g}) \simeq 2u_K. \tag{2.10}$$

Eq. (2.7) then becomes

$$0 = -\eta\frac{u_K^2}{r} + \frac{2u_K}{r}\left(u_{\phi,d} - u_{\phi,g}\right) - \frac{1}{t_s}\left(u_{r,d} - u_{r,g}\right), \tag{2.11}$$

so if we finally substitute Eq. (2.9) into Eq. (2.11), after some passages, we find the radial velocity of the particle to be

$$u_{r,d} = \frac{\tau_s^{-1} u_{r,g} - \eta u_K}{\tau_s + \tau_s^{-1}} = \frac{u_{r,g}}{1+\tau_s^2} - \frac{2u_{r,n}}{\tau_s + \tau_s^{-1}}. \tag{2.12}$$

[1] In fact we can write the net acceleration in the radial direction as follows

$$\frac{du_{r,d}}{dt} = u_{r,d}\frac{du_{r,d}}{dr}.$$

We also know that, for the gas, it is true that

$$u_{r,g} \sim \frac{\nu}{r} \sim \alpha c_s \left(\frac{H_p}{r}\right) \ll c_s,$$

allowing the neglection of the term $u_{r,g}(du_{r,g}/dr)$ by virtue of the fact that the local Kepler velocity in a thin disk is highly supersonic. Similarly, if the dust particles follow nearly circular orbits close to Keplerian motion, the term $u_{r,d}(du_{r,d}/dr)$ can be neglected if it holds $u_{r,d} \ll c_s$.

We have separated the addition into two terms on purpose: the first term is the drag term coming from the radial movement of the gas at velocity $u_{r,g}$, which is able to partially drag the dust along on a rate depending on the level of coupling between the two. The second term is the radial drift velocity with respect to the gas $u_{r,\text{drift}}$, which represents the effect of the so called "head wind". Here we follow Birnstiel, Dullemond and Brauer (2010), [20], defining $u_{r,n}$ as follows

$$u_{r,n} = -E_d \cdot \frac{1}{2\Omega_K} \frac{1}{\rho_g} \frac{\partial P}{\partial r}, \tag{2.13}$$

with the physical meaning of the maximum drift velocity of a particle (Weidenschilling, 1977, [18]). Here E_d is a radial drift efficiency parameter describing how efficient the radial drift actually is, as several mechanism such as zonal or meridional flows might occur.
Furthermore we point out that, in the above derivation of Eq. (2.12), we assumed that in the z-direction the particle sedimentation is balanced by the turbulent diffusion (a vertical equilibrium), but that in the r-direction the turbulent effects are neglected. We shall see how to consider the turbulence effect soon.
Now we can consider the special cases of Eq. (2.12):

i) $\tau_s \ll 1$: for particles well coupled with the gas the radial velocity reduces to

$$u_{r,d} = u_{r,g} + u_{r,\text{drift}} = u_{r,g} - \eta\tau_s u_K,$$

so that they experience a radial drift relative to the gas at a rate which is linear in τ_s. To a good approximation the dust's azimuthal velocity will equal the sub-Keplerian velocity of the gas, yet being devoid of the balance of radial pressure: hence the particle will spiral inward;

ii) $\tau_s \gg 1$: for large particles decoupled from the gas the radial motion of the gas does not affect the particles' velocity, so that

$$u_{r,d} = -\eta\tau_s^{-1} u_K,$$

which conversely decrease linearly with τ_s. The particles orbits the central mass with an azimuthal velocity that is close to the Keplerian speed, hence faster than the motion of the gas, therefore experiencing an effect known as "head wind", which saps their angular momentum.

The explicit expression of τ_s depends on the appropriate aerodynamic regime. For small grains we can either have Epstein and Stokes regime, while for larger particles $\lambda_{\text{mfp}} \lesssim a$.
Eq. (2.12) peaks when $\tau_s \sim 1$ at the value

$$u_{r,d}^{\max} = -\frac{1}{2}\eta u_K. \tag{2.14}$$

We have plotted in Fig. (2.1) the ratio between the radial drift velocity at the mid-plane and u_K as function of τ_s. In Fig. (2.2) the same quantity's dependence on the dust particle radius a is shown.

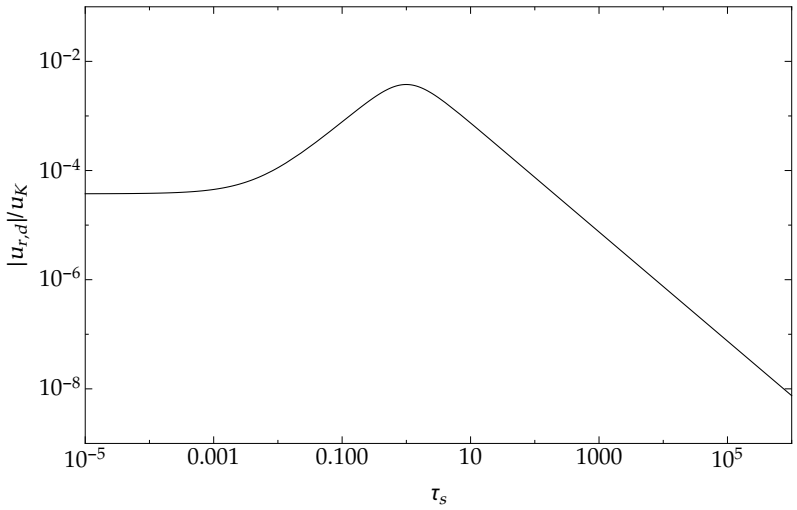

Figure 2.1: The radial drift velocity at the mid-plane in units of u_K as a function of the dimensionless stopping time $\tau_s = \Omega_K t_s$. We assumed reasonable values at 5 AU, i.e. $\eta = 7.5 \times 10^{-3}$, $H_p/r = 0.05$, and also that $u_{r,g}/u_K = -3.75 \times 10^{-5}$.

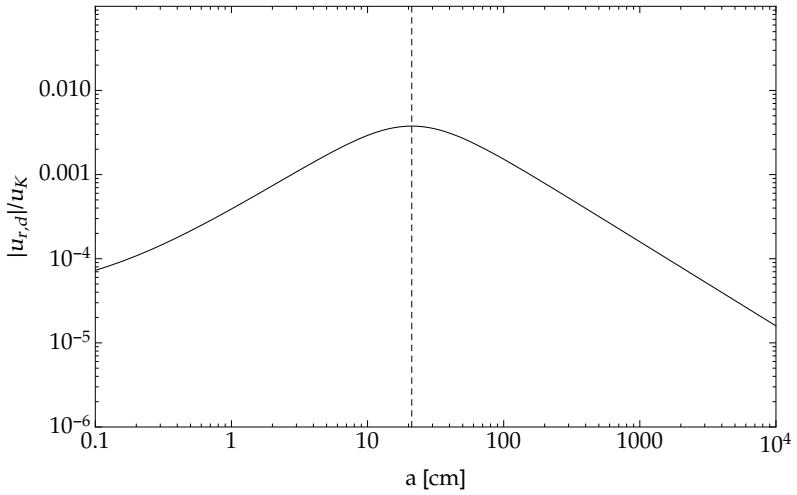

Figure 2.2: The radial drift velocity at the mid-plane in units of u_K as a function of the dust particle radius a. We assumed the same reasonable values at 5 AU written above, and the vertical dotted line indicate the maximum of the curve, i.e. at $a \simeq 21$ cm.

Let us now make an estimate on appropriate conditions at the mid-plane at 5 AU (Armitage, 2010, [21]), i.e. $\Sigma_g = 10^2$ g cm^{-2} and $H_p/r = 0.05$. Recalling Eq. (2.6), a dimensionless stopping time of unity occurs when

$$a = \left.\frac{\rho_g \bar{u}}{\rho_s \tau_s \Omega_K}\right|_{\tau_s=1} = \frac{\rho_g}{\rho_s}\left(\frac{8}{\pi}\right)^{1/2}\frac{H_p}{r}\,r = \frac{\Sigma_g}{\rho_s}\left(\frac{2}{\pi}\right) \simeq 21 \text{ cm},$$

which is typical in the inner disk (from 1 AU to 10 AU), where the peak of Eq. (2.14) is reached by particles of size from 10 cm to few meters. Defining

the *minimum radial drift* time scale

$$t_{\rm drift}^{\rm min} \equiv \frac{r}{|u_{r,d}^{\rm max}|}, \tag{2.15}$$

we can understand the order of magnitude with the reasonable at 5 AU values used above, and $c_s \sim 10^5\,{\rm cm\,s^{-1}}$, as follows

$$t_{\rm drift}^{\rm min} = r \cdot \left[\frac{1}{2}\eta\left(\frac{r}{H_p}\right)c_s\right]^{-1} = \frac{2r}{\eta}\left(\frac{H_p}{r}\right)\frac{1}{c_s} \lesssim 10^2\,{\rm yr},$$

which is extremely short. Hence we conclude that planetesimals formation must be very rapid, otherwise the fast radial drift toward the central star would efficiently drive the vast majority of solids to evaporate near the hot inner regions of the protoplanetary disk. This is commonly referred to as the *"meter size barrier"*, because of the extraordinary low values of $t_{\rm drift}^{\rm min}$ reached by bodies of size $10\,{\rm cm} \lesssim a \lesssim 1\,{\rm m}$, and how to overcome radial drift remains an unsolved problem.

Let us now consider the effects of the turbulence in the radial dynamics of the dust, which was previously manifestly neglected. We will not consider the accretional evolution of the disk in this treatment.
If the disk is turbulent, in effect, small dust particles that are aerodynamically well coupled to the gas will diffuse radially (and also vertically, as we shall see in section 2.3) to equalize the concentration relatively to the dominant gaseous component. Defining the concentration of the dust (treating it as a fluid "contaminant" with respect to the gas) $\mathcal{S}$ as follows

$$\mathcal{S} = \frac{\Sigma_d}{\Sigma_g},$$

where we named Σ_d the surface density of the dust, the overall movement of Σ_d can be described by an advection-diffusion equation:

$$\frac{\partial \Sigma_d}{\partial t} + \nabla \cdot \mathbf{F_{tot}} = 0 \quad \Rightarrow \quad \frac{\partial \Sigma_d}{\partial t} + \frac{1}{r}\frac{\partial}{\partial r}\left(rF_{tot}\right) = 0, \tag{2.16}$$

In Eq. (2.18) we see at the right the general continuity equation, which implies that the dust is neither created or destroyed locally in the disk, and at the left the component of the equation we are interested in, i.e. the radial one. The total flux $F_{\rm tot}$ is expressed by the two components of diffusive and advective flux,

$$\mathbf{F_{tot}} = \mathbf{F_{adv}} + \mathbf{F_{diff}} = \Sigma_g \mathbf{u_d} - D\,\nabla\left(\frac{\Sigma_d}{\Sigma_g}\right)\cdot\Sigma_g, \tag{2.17}$$

$$\Rightarrow F_{\rm tot} = \Sigma_d u_{r,d} - D\left(\frac{\partial}{\partial r}\mathcal{S}\right)\cdot\Sigma_g,$$

where D is the turbulent diffusion coefficient, expressing the ratio of dust diffusivity; it is often taken as $D \sim \nu$. So the time dependent equation for the surface density of one dust species of mass m_i is given by

$$\frac{\partial \Sigma_d^i}{\partial t} + \frac{1}{r}\frac{\partial}{\partial r}\left\{ r \cdot \left[\Sigma_d^i \cdot u_{r,d}^i - D^i \frac{\partial}{\partial r}\left(\frac{\Sigma_d^i}{\Sigma_g}\right) \cdot \Sigma_g \right] \right\} = S_d^i, \tag{2.18}$$

where a source term S_d^i is included to account for re-condensation of grains or dust evaporation and outflows (Birnstiel, Dullemond and Brauer, 2010, [20]).

2.3 Vertical settling

We will now investigate the effect of the aerodynamic forces on the vertical distribution, once again neglecting the turbulence at first. Let us consider the forces acting on a spherical grain of mass m above the mid-plane at height z of a laminar disk: the vertical component of the gas drag and the gravity, counteracting each other, such the particle at rest will accelerate downwards. The z-component of the equation of motion hence is

$$m\frac{\partial u_{z,d}}{\partial dt} = \frac{GM_* mz}{(r^2+z^2)^{1/2}} + F_{D,z}$$

$$m\frac{\partial u_{z,d}}{\partial dt} = -\Omega_K^2 mz - \frac{4}{3}\pi \rho_g a^2 \bar{u} \Delta u_z, \tag{2.19}$$

where Δu_z is the vertical relative velocity and we have used the usual thin disk approximation $H_p/r \ll 1$ and substitute the Epstein drag law Eq. (2.2). Setting the equilibrium in Eq. (2.19), we obtain the settling speed u_{settle}:

$$u_{\text{settle}} = -\frac{3}{4}\left(\frac{m}{\sigma}\right)\frac{\Omega_K^2 z}{\rho_g \bar{u}} = -\frac{a}{\bar{u}}\left(\frac{\rho_s}{\rho_g}\right)\Omega_K^2 z. \tag{2.20}$$

Settling is hence more rapid at higher heights, where the gas density is lower and the vertical component of gravity stronger, and also for larger grains. We can make an order of magnitude estimate defining the settling time scale t_{settle} as follows

$$t_{\text{settle}} \equiv \frac{z}{|u_{\text{settle}}|}, \tag{2.21}$$

and using reasonable values for a 1 μm at 1 AU at height $z = h$, (from [21], $\rho_g = 5 \times 10^{-10}$ g cm^{-3}, $\rho_s = 3$ g cm^{-3}, $\bar{u} = 2.4 \times 10^5$ cm s^{-1}, $H_p/r = 0.05$), obtaining

$$t_{\text{settle}} = h \cdot \left[\frac{a}{\bar{u}}\left(\frac{\rho_s}{\rho_g}\right)\Omega_K^2\right]^{-1} = \frac{1}{\bar{u}}\frac{\rho_g}{\rho_s}\left(\frac{H_p}{r}\right)^2 \frac{8}{\pi}\frac{r^2}{a} \approx 1 \times 10^5 \text{ yr},$$

which is short in comparison with the disks' lifetimes. Inserting the expression for the vertical density profile of a vertically isothermal disk ρ_g from Eq. (1.3), the general expression for the settling time scale becomes

$$t_{\text{settle}} = \frac{16}{\pi^2}\frac{\Sigma_g}{\rho_s\, a\, \Omega_K} e^{-z^2/2H_p^2},$$

by which we can say that settling becomes rapid and rapid as the height z increases, in absence of turbulence.

We can now consider the effect of turbulence in vertical settling, which counteracts settling grains stirring them up and preventing them to accumulate in a thin layer on the mid-plane. The effect is mostly efficient on the small particles well coupled to the gas, i.e. with $\tau_s \ll 1$. We will neglect radial migration of the grains due to gas drag or other effects, together with the accretional evolution of the disk.
We write the density function of grains located at height z above the midplane and at distance r to the star at the time t as $\rho_d(m, r, z, t)$. Treating again the dust as a fluid "contaminant" with respect to the gas, $\rho_d \ll \rho_g$, the dust density obeys an advection-diffusion equation (Dubrulle, Morfill & Sterzik, 1995 [22]; Fromang & Papaloizou, 2006 [23]) such as Eq. (2.16), where the total flux $F_{\rm tot}$ can be written from Eq. (2.17) as follows

$$\mathbf{F_{tot}} = -\rho_d \mathbf{u_d} - D\,\nabla\left(\frac{\rho_d}{\rho_g}\right)\cdot\rho_g,$$

$$\Rightarrow F_{\rm tot} = -\Omega_K^2 t_s \rho_d z - D\left(\frac{\partial}{\partial z}\,\frac{\rho_d}{\rho_g}\right)\cdot\rho_g,$$

where we have written the z-component of the flux and used the equation of motion Eq. (2.19) together with the definition of Eq. (2.4). So the time dependent equation for the dust density of one dust species of mass m_i, called the settling-stirring equation, is

$$\frac{\partial \rho_d^i}{\partial t} = \frac{\partial}{\partial z}(\Omega_K^2 t_s \rho_d z)^i + \frac{\partial}{\partial z}\left[D\frac{\partial}{\partial z}\left(\frac{\rho_d^i}{\rho_g}\right)\cdot\rho_g\right], \tag{2.22}$$

where the density function of grains $\rho_d^i(r, z, t)$ is calculated at a specific value of r.

* * *

Chapter 3

Coagulation

As anticipated, the formation of planetesimals is typically framed in the scenario of incremental growth, in which the process starts with micron-sized dust particles colliding and sticking together by surface forces to form larger aggregates. The next stage in the formation process is the gravity-aided regime, where the formed planetesimals are so massive that the gravity will provide the force keeping the bodies together.
Collisions can occur between bodies of different sizes and composition as well as at different relative velocities. While the existence of planets seems to indicate that, on average, collisions lead to growth, it is quite possible that a collision leads to destruction, the survival of a growing object resting on the probability that it will not be subjected to a collisional energetic enough to destroy itself in its lifetime.

In the following sections we shall describe the collisional growth, called *coagulation* for small dust particles, proposing a basic analytical treatment through the Smoluchowski equation and some order of magnitude estimates too. Coagulation, in fact, deeply affects the general dust evolution mechanism explained in the previous chapter, and it will be our purpose to investigate these effects. We will also point out the roots of the main challenge of theories of planetesimals formation: the physical limitation in growth of aggregates due to the (already encountered) meter size barrier together with fragmentation counteracting growth.
We shall underline that we will always assume the dust particles to have a constant in time volume density ρ_s and to be compact spheres, as done untill now, not tracing the evolution of porosity of the particles at all for it will be far beyond our scopes.

3.1 Smoluchowski equation

We will start with an analytical approach to the coagulation paradigm, following the now-classic Smoluchowski argument (Smoluchowski, 1916 [24]) according to which a simple, discrete equation can be used to describe the collisional growth at small sizes. We shall develop later this ansatz with a more recent model by Birnstiel & Dullemond (see [20], 2010, or also [25], 2005).

The simplest form of a coagulation equation can be written as follows, assuming that the masses of dust particles are integral multiples of an elementary mass m_1 and at a given time t there are n_k bodies of mass $m_k = km_1$:

$$\frac{dn_k}{dt} = \frac{1}{2}\sum_{i+j=k} K_{i,j} n_i n_j - n_k \sum_{i=1}^{\infty} K_{k,i} n_i, \tag{3.1}$$

where $K_{i,j}$ is the interaction kernel between bodies of mass m_i and mj. The meaning of the right hand side terms is quite clear: the first term represents the growth in the number of bodies of mass m_k due to collisions of all possible pairs of particles with masses m_i and m_j which sum up to m_k; the second term represents the decrease due to bodies of mass m_k being used to form larger bodies. We reserve to give a proper definition of the kernel later in this section.

Let us now progressively develop this model: due to the enormous number of mass bins necessary to treat the coagulation equation in its discrete variant, we would rather describe the population of dust grains with a continuous dust grain distribution $n(m, r, z, t)$, which is a function of mass m, distance to the star r and height z above the mid-plane at the time t. It describes the number of particles per cm^3 per gram interval in particle mass, such that the total dust density $\rho_d\,(m, r, z, t)$ in $\mathrm{g\,cm}^{-3}$ is given by

$$\rho_d\,(m, r, z, t) = \int_0^{\infty} n(m, r, z, t) \cdot m\, dm. \tag{3.2}$$

The collisional time evolution of this quantity $n(m, r, z, t)$ is then described as a general two-body process by the integral form of the coagulation equation Eq. (3.1):

$$\begin{aligned}\frac{\partial n(m, r, z, t)}{\partial t} = \int \int_0^{\infty} A(m, m', m'') \cdot n(m', r, z, t) \times \\ \times\, n(m'', r, z, t)\, dm'\, dm'',\end{aligned} \tag{3.3}$$

where $A(m, m', m'')$ is the so called reaction kernel, with m being the analogous of the elementary mass m_k and m_i, m_j are now plainly indexed. The dependence of $A(m, m', m'')$ on the radius, height above the mid-plane and time are hereafter omitted for simplicity. The reaction kernel A is defined relying on the simple form given by Eq. (3.1) by means of the coagulation kernel $K(m', m'')$:

$$A(m, m', m'') = \frac{1}{2} K(m', m'') \delta(m' + m'' - m) - K(m', m'') \delta(m'' - m), \tag{3.4}$$

with $K(m', m'')$ covering the same role as the discrete coagulation kernel $K_{i,j}$. The expression Eq. (3.3) can be rather unenlightening, so we will use the Dirac δ function properties to write a more explicit version of the coagulation equation:

$$\frac{\partial n(m,r,z,t)}{\partial t} = \frac{1}{2}\int_0^m K(m-m',m',t)\cdot n(m-m',r,z,t)\cdot n(m',r,z,t)\,dm' -$$

$$- \; n(m,r,z,t)\int_0^\infty K(m,m',t)\cdot n(m',r,z,t)\,dm', \tag{3.5}$$

where it is now clear that the first term on the right hand side is the source term for the formation of mass m particles from coagulation of $(m-m')+m$ particles, while the second term is the sink term due to the incorporation of m by collisions with m'. The factor of one half eliminates double counting of the collisions that increases the number of particle of mass m.
Let us finally define the general form of the coagulation kernel $K(m_1, m_2)$, with m_1 and m_2 being the masses involved in the reaction, which encloses all the physics of the process. In our case it can be written as the following product of three factors:

$$K(m_1,m_2) = \Delta u(m_1,m_2)\sigma_c(m_1,m_2)P_k(m_1,m_2,\Delta u).$$

Here $P_k(m_1, m_2, \Delta u)$ is the probability that a collision between two particles of mass m_1 and m_2 leads to adhesion, $\Delta u(m_1, m_2)$ is the relative velocity of the two particles and $\sigma_c(m_1, m_2)$ is the geometrical cross section of the collision. We shall underline that all these factors can also depend on other material properties such as shape or porosity, however we shall not deepen the issue as stated before.

Up to now we have discussed the coagulation process implicitly assuming that the collisions between particles lead successfully to sticking growth. However this is not necessarily true: as we shall see later, for sufficiently high relative collision velocities the aggregates may fragment into smaller bodies. Hence we need a straightforward generalisation of the Smoluchowski equation Eq. (3.3) to account for fragmentation mechanism. We follow Dullemond & Dominik (see [20]) for this purpose, as it is sufficient to redefine the reaction kernel as follows

$$A(m,m',m'') = \frac{1}{2}K(m',m'')\cdot\delta(m'+m''-m) - K(m',m'')\cdot\delta(m''-m) +$$

$$+ \frac{1}{2}F(m',m'')\cdot S(m,m',m'') - F(m',m'')\cdot\delta(m-m''),$$

where $F(m', m'')$ and $S(m, m', m'')$ are the fragmentation kernel and the distribution of fragments function. Hence the third term represents the fragmentation of masses m and m' governed by $F(m', m'')$, and the fourth account for the fact that, when masses m and m' fragment, they distribute some of their

mass via fragments to smaller sizes. The fragmentation kernel can be similarly written as three factors

$$F(m_1, m_2) = \Delta u(m_1, m_2)\sigma_c(m_1, m_2)P_f(m_1, m_2, \Delta u),$$

where $P_f(m_1, m_2, \Delta u)$ is the fragmentation probability, which is still not well known and usually taken with a simple form (following Dullemond, Brauer, Henning, 2008, [26])

$$P_f(m_1, m_2, \Delta u) = \left(\frac{\Delta u}{u_c}\right)^{\psi} \Theta(u_c - u) + \Theta(u - u_c).$$

Here the two Heaviside step functions Θ ensure that the particles fragment with unitary probability if the relative particle velocity $\Delta u(m_1, m_2)$ is larger than a critical fragmentation velocity u_c; while for $\Delta u(m_1, m_2) < u_c$ we assume that there is always a possibility for fragmentation given by $(\Delta u/u_c)^{\psi}$, with a free parameter ψ. The particle distribution $S(m, m', m'')$ after fragmentation is usually described by a power-law such that

$$n(m)\, dm \propto m^{-\xi}\, dm$$

where $n(m)dm$ is the number of particles per unit volume within the mass range $[m, m + dm]$, and ξ accounts for the efficiency of the fragmentation process: its value is been investigated through both theoretical and experimental studies, the latter ones (see Blum, Munch, 1993 [27]) with results ranging from 1.3 (low velocity impacts) and 2 (catastrophic impacts).

We will add that, in the case where masses of colliding particles differ by orders of magnitude, a complete fragmentation scenario is quite unrealistic, and the cratering phenomenon is usually thought more likely: a smaller body will excavate a certain amount of mass from a larger one, and the amount of mass removed can be parametrized in units of the smaller body m_s as

$$m_{\rm rem} = \chi\, m_s.$$

The mass of the smaller particle,together with the mass excavated from the larger one, is then redistributed according to the power law distribution of fragments (Sirono, 2004, [28]).
It is worth noticing the importance of the relative velocities between interacting particles $\Delta u(m_1, m_2)$ in defining the kernels and the physics: the sources of Δu will be the subject of the following section.

It is lastly evident that the coagulation of grains expressed by Eq. (3.3) is a one dimensional time-dependent problem in m, which has to be solved at each r and z. In order to give an idea of a more complete analytical formulation of the physics of coagulative processes, we would like to include in the equation the effects of the turbulent mechanisms encountered in the previous chapter: the settling-stirring dynamic Eq.(2.22) and the radial drift equation Eq. (2.18).

i) *Coagulative settling-stirring*
The problem of dust settling and stirring lives in the coordinate z, while coagulation is a problem in the coordinate m: we want to solve them simultaneously with a self-consistent model, following Dominik & Dullemond (2004b, [29]).
Let us recall that the definition given above for the distribution function of dusty particles, $n(m, r, z, t)$, is such that $n(m, r, z, t)\, m\, dm$ is a dust mass density in g cm^{-3}, the total dust density $\rho_d(m, r, z, t)$ given by

$$\rho_d\,(m, r, z, t) = \int_0^\infty n(m, r, z, t) \cdot m\, dm.$$

It is hence possible to reconstruct an advection-diffusion equation for the distribution function $n(m, r, z, t)$ at fixed radius r, i.e. a settling and vertical mixing equation, and thus formulating a consistent coagulative problem accounting for this turbulent effect:

$$\frac{\partial n(m, z, t)}{\partial t} = \int\int_0^\infty A(m, m', m'') \cdot n(m', z, t) \cdot n(m'', z, t)\, dm'\, dm'' +$$

$$+ \frac{\partial}{\partial z}(n(m, z, t) \cdot u_{\rm settle}) + \frac{\partial}{\partial z}\left[D\frac{\partial}{\partial z}\left(\frac{n(m, z, t)}{\rho_g}\right) \cdot \rho_g\right],$$

where $u_{\rm settle}$ is the usual settling velocity obtained from the vertical equation of motion Eq. (2.19), and the radial dependence is here eliminated since the resolution has to be thought at fixed radius r, i.e. particles are not allowed to move from one vertical slice to another in this formulation.

ii) *Coagulative radial turbulent drift*
Now we have a problem in the radial coordinate, to be coniugated with the coagulation problem in m coordinate. For this purpose we shall point out that the dusty particles density distribution $n(m, r, z, t)$ is defined such that $n(m, r, z, t)m\, dm\, dz$ represents the number of grains of size m and at height z per unit area of disk, giving for the total dust surface density the following expression

$$\Sigma_d(m, r, t) = \int\int_{-\infty}^\infty n(m, r, z, t) \cdot m\, dm\, dz.$$

If we now define the vertically integrated dust surface density distribution per gram intervals $\sigma_d(r, t)$ as follows

$$\sigma_d(m, r, t) \equiv \int_{-\infty}^\infty n(m, r, z, t) \cdot m^2\, dz,$$

it is then analogously possible to reconstruct an advection-diffusion equation for the distribution function $n(m, r, z, t)$ at fixed height z, i.e. an

equation for the radial turbulent drift, formulating again a consistent coagulative problem accounting for this turbulent effect:

$$\frac{\partial \sigma_d(m,r,t)}{\partial t} = \int\int_0^\infty A(m,m',m'') \cdot \sigma_d(m',r,t) \cdot \sigma_d(m'',r,t)\, dm'\, dm'' -$$

$$- \frac{1}{r}\frac{\partial}{\partial r}\left[r \cdot \sigma_d(m,r,t) \cdot u_{r,d}\right] + \frac{1}{r}\frac{\partial}{\partial r}\left[r \cdot D\left(\frac{\sigma_d(m,r,t)}{\Sigma_g}\right) \cdot \Sigma_g\right],$$

where $u_{r,d}$ is the usual radial velocity discussed in section (2.2).

We can easily conclude pointing out that the continuous formulation of the coagulation equation corresponds to a non linear integro-differential equation, resulting difficult to solve even in its discrete version, unless a choice of very simple (and rather unphysical) kernels. Hence the necessity of solving coagulation equation numerically, which represents a great importance issue of the last decades studies.

3.2 Relative particles velocity

The aim of this section is to investigate the sources of the relative particles velocity Δu, which is the key term for the physics of the (coagulative) interacting process.
We shall keep in mind that whether planetesimals can form via coagulation depends upon how frequently do particles collide and also on what is the outcome of the collision, since, as we pointed out in the previous section, a sticky collision has not a 100% probability of success. We need hence to define the collision time scale t_{collide} for a population of compact spherical particles of mass m with radius a and solid density ρ_s:

$$t_{\text{collide}} \equiv \frac{1}{n_d \sigma_c \Delta u}, \tag{3.6}$$

where σ_c is the cross section for collision, being equal to $\sigma_c = \pi(2a)^2$ for a spherical dust grain, and n_d is the particle number density, which can be calculated as

$$n_d = f\,\frac{\rho_g}{m},$$

with f being the usual gas-to-dust ratio (untill now taken approximately constant $f \sim 0.01$, which is only partially true). Determining the appropriate value of Δu is therefore crucial in order to make some order of magnitude estimates of t_{collide}. It is worth noticing that σ_c is substantially different from σ used in the aerodynamic relationships: the first is the cross section for collisions between two grains of equal radius a, while the second was the gas-grain collision cross section, $\sigma = \pi a^2$.

There are various sources of relative velocities between interacting particles, and we shall consider the following: Brownian motion, differential settling, azimuthal relative velocity, radial drift and turbulence, keeping for later some estimates of these effects where possible.

i) *Brownian motion*
Let us distinguish again the particle's masses m_i and radii a_i for clarity. From thermodynamic theory we should know that two particles of mass m_1 and m_2 in a region of the disk in thermal equilibrium with a gas at temperature T have an average statistical relative velocity due to Brownian motion, given by

$$\Delta u_{\rm BM}(m_1, m_2) = \sqrt{\frac{8k_B T(m_1 + m_2)}{\pi m_1 m_2}}, \tag{3.7}$$

representing an average of random velocities which is highest when both particles have the smallest mass. Therefore, Brownian motion favors collisions in which at least one collision partner has low mass.

ii) *Differential settling*
Differential settling is the process by which large grains, which settle faster than small grains, sweep up the smaller grains on their way to the mid-plane. We shall deepen this issue in the next section. This mechanism introduce a systematic relative velocity term given by

$$\Delta u_{\rm DS}(m_1, m_2) = |u_{\rm settle}(m_1) - u_{\rm settle}(m_2)|,$$

where $u_{\rm settle}$ is the usual equilibrium settling speed discussed in section (2.3), which corresponds to $u_{\rm settle} = -\Omega_K^2 t_s z$ for particles in the Epstein regime. In this particular regime hence we have

$$\Delta u_{\rm DS}(m_1, m_2) \propto \left| z_1 \cdot \left(\frac{m_1}{\sigma_1}\right) - z_2 \cdot \left(\frac{m_2}{\sigma_2}\right) \right|,$$

where $\sigma_{c,i} = \pi a_i^2$ are the gas-grain collision cross sections for particles of radius a_i. This contribution is clearly zero for particles with equal (m/σ) ratios, meaning that the relative velocity is zero for equal mass particles for they both settle at equal speed. The differential settling as a source of collisions works hence best for particles of very different mass-to-crosssection ratios, leading therefore to largest mass aggregates sweeping up the smallest particles.

iii) *Differential radial drift*
The radial drift causes relative velocities between particles since particles of different sizes couple differently to the surrounding gas. The relative velocity contribution is simply

$$\Delta u_{\rm RD} = |u_{r,d}(m_1) - u_{r,d}(m_2)|,$$

where the radial velocity of the dust $u_{r,d}$ is given by Eq. (2.12) in different regimes.

iv) *Azimuthal relative velocities*
The azimuthal relative velocities occur for the same reasons as the radial drift, and are induced by the azimuthal gas drag. According to Dullemond & Dominik (see [20]), while only particles around $\tau_s = 1$ are significantly drifting, relative azimuthal velocities do not vanish for encounters between very large and very small particles instead. This contribution can be written as follows

$$\Delta u_{\phi,d} = |u_{\phi,d}(m_1) - u_{\phi,d}(m_2)|,$$

where the azimuthal drift of a particle $u_{\phi,d}$ is calculated from the equations of motion discussed in section (2.2):

$$u_{\phi,d} = \frac{\eta u_K}{1+\tau_s^2} = \frac{u_{r,n}}{1+\tau_s^2} \quad \Rightarrow \quad \Delta u_{\phi,d} = \left| u_{r,n} \cdot \left(\frac{1}{1+\tau_{s_1}^2} - \frac{1}{1+\tau_{s_2}^2} \right) \right|$$

with the usual maximum drift velocity $u_{r,n}$ defined in Eq. (2.13), and the dimensionless stopping time τ_{s_i} are referred to the relative particles of mass m_i.

v) *Turbulent motion*
Turbulence-driven coagulation is a rather complex process, since it arises from MRI, and its effect on the dust motion can roughly be divided into different regimes depending on how well coupled the particle is to the gas. We shall not deepen this issue, calling Δu_T the contribution to the relative velocity due to this phenomenon.

The total relative velocity Δu is hence the root of the squared sum of all these terms:

$$\Delta u = \sqrt{\Delta u_{\mathrm{BM}}^2 + \Delta u_{\mathrm{DS}}^2 + \Delta u_{\mathrm{RD}}^2 + \Delta u_{\phi,d}^2 + \Delta u_T^2}. \tag{3.8}$$

Let us now make some estimates. We shall investigate the typical collision time scale t_{collide} in the simple assumption of "hit-and-stick" model for collisional growth, not discussing the outcome of the interaction, but keeping in mind that other mechanisms, such as fragmentation or cratering, may also occur.
In the case where all the particles have the same mass, $m_1 = m_2 = m$, and considering small dust grains, we can describe their relative velocities as mostly due to Brownian motion, since they are well coupled to the gas particles:

$$\Delta u = \Delta u_{\mathrm{BM}} = \sqrt{\frac{16 k_B T}{\pi m}}.$$

Inserting this value in the definition of t_{collide}, Eq. (3.6), and recalling that $m = 4/3\pi\rho_s a^3$, we obtain

$$t_{\mathrm{collide}} = \frac{m}{f\rho_g} \cdot \left(\frac{1}{\sigma_c}\right) \sqrt{\frac{\pi m}{16 k_B T}} = \frac{\pi}{6\sqrt{3}} \cdot \left(\frac{1}{f\rho_g}\right) \frac{a^{5/2}\rho_s^{3/2}}{\sqrt{k_B T}}. \tag{3.9}$$

Substituting now typical values for conditions in the inner protoplanetary disk, e.g. at 1 AU ($\rho_g = 10^{-10}\,\mathrm{g\,cm^{-3}}$, $f \sim 0.01$, $\rho_s = 3\,\mathrm{g\,cm^{-3}}$, $T = 300\,\mathrm{K}$), Eq. (3.9) yields

$$t_{\mathrm{collide}} \simeq 8 \left(\frac{a}{1\ \mu\mathrm{m}} \right)^{5/2} \mathrm{yr},$$

which is extremely short, suggesting that, if Brownian motion is the only non negligible source of relative velocity, the collisions are very rapid. So, if our hypothesis of sticky collisions is true, growth of aggregates must be fast. On the other hand, if we calculate Δu_{BM} in the above conditions taking into account micrometer sized and centimeter sized particle, the results are particularly interesting:

$$\Delta u_{\mathrm{BM}}(a \sim \mu\mathrm{m}) = 0.1\,\mathrm{cm\,s^{-1}}, \quad \Delta u_{\mathrm{BM}}(a \sim \mathrm{cm}) = 1.3 \times 10^{-7}\,\mathrm{cm\,s^{-1}},$$

which is a simple example showing that there is practically no coagulation due to Brownian motion for particles much larger than micrometer size.
Similarly we can also obtain a relevant expression for the rate of growth da/dt:

$$\frac{dm}{dt} = \sigma_c \left| \Delta u_{\mathrm{BM}} \right| f \rho_g(z) \quad \Rightarrow \quad \frac{da}{dt} = f \left(\frac{\rho_g}{\rho_s} \right) \sqrt{\frac{16 k_B T}{\pi m}}, \tag{3.10}$$

where the vertical isothermal structure of the disk ρ_g is given by Eq.(1.3). At the mid-plane, an elementary integration of Eq. (3.10) gives the following analytical profile for the rate of growth of particle radius a:

$$a(t) = \left(\frac{5}{2} \frac{\rho_d}{\rho_s \pi} \sqrt{\frac{12 k_B T}{\rho_s}} (t - t_0) + a_0^{5/2} \right)^{2/5}.$$

This profile is plotted in Fig. (3.1), with the above adopted parameters for the inner regions of the disk, at different initial values of the radius a_0. From the figure it is evident the very rapid growth due to Brownian motion-induced collisions for particles of sub-micrometer size, which reach a micrometer radius in a time $t \lesssim 10^4$yr. The particles with an initial radius $a_0 \sim \mu$m are showed to have a quite slow growth, but we have to keep in mind that, in this calculation, only the Brownian motion is taken into account as a source of relative velocities enhancing sticky collisions.

For larger particles the relative velocity is then to be considered as the sum of more than one (or all) term of the Eq.(3.8), such as differential motion or velocity induced by turbulence within the disk, decreasing more or less efficiently the collision time scale. Anyway we can say that the collision frequency is high enough that growth up to the μm size regime presents no time scale problems with respect the disks' lifetime. We shall see, in the following section, that this is generally true even up to cm sizes.

Let us now lastly consider a population of boulders of size $a = 1\,\mathrm{m}$. For these consistently larger aggregates the relative velocity is dominated by radial drift

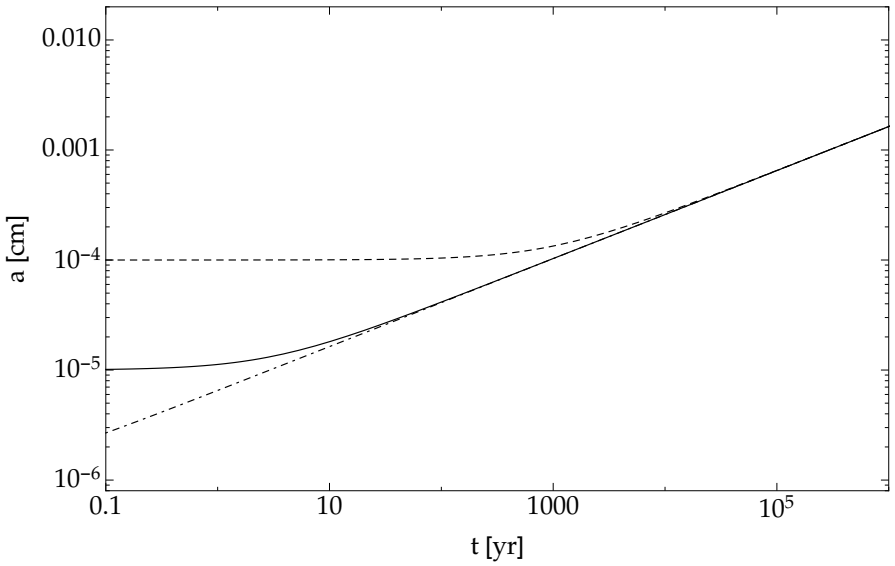

Figure 3.1: The rate of growth of the particle radius da/dt for three different values of the initial size a_0 and for the initial time $t_0 = 0$. From top to bottom the curves are about $a_0 = 1\,\mu$m (dashed), $a_0 = 0.1\,\mu$m (solid) and $a_0 = 0.01\,\mu$m (dot-dashed). The parameters adopted are typical for conditions in the inner protoplanetary disk, i.e. $\rho_g = 10^{-10}\,\mathrm{g\,cm^{-3}}$, $f \sim 0.01$, $\rho_s = 3\,\mathrm{g\,cm^{-3}}$, $T = 300\,\mathrm{K}$.

due to the aerodynamic forces in the surrounding gas. The collision time scale can be written as

$$t_{\mathrm{collide}} = \frac{m}{f\rho_g} \cdot \left(\frac{1}{\sigma_c}\right) \frac{1}{\Delta u} = \frac{1}{3}\frac{\rho_s}{\rho_g}\frac{a}{\Delta u},$$

which, adopting reasonable parameter values at 1 AU ($\Delta u \sim 10^{-3}\, u_K \sim 3 \times 10^3\,\mathrm{cm\,s^{-1}}$), yields for $f = 0.01$

$$t_{\mathrm{collide}} \sim 10^3\,\mathrm{yr},$$

a very short time scale which still exceeds the estimate of $t^{\mathrm{min}}_{\mathrm{drift}}$ given in section (2.2), i.e. the time needed by radial drift to cause boulders of this size to migrate toward the central star. It is thus evident from these simple argumentations too that the so called meter size barrier represents a theoretical obstacle, which is yet to overcome. For what we know, a coagulation model of growth fails from centimeter to meter size aggregates, being very efficient for smaller particles instead. The fact that these larger scales are not readily accessible to laboratory experiments adds significantly to the difficulties.

3.3 Differential settling and radial drift

We will now investigate the effects of adhesive collisions on the vertical settling and the radial drift encountered in sections (2.3) and (2.2). In the previous

chapter we decribed these dynamic processes taking into account the turbulence via advection-diffusion equations: we will neglect disk's turbulence here, aiming at a simple description of the coagulative growth in the z and r directions.

As we have anticipated, the process in which large particles, settling faster vertically toward the mid-plane, collide and, possibly, stick with the encountered smaller particles is called differential settling. We will follow a classic idea by Safronov (1969, [30]) in order to make an estimate of how efficiently a dust grain could grow during sedimentation.
Let us consider a single dust particle of radius a and solid density ρ_s settling in a disk, assuming that all the other dust particles remain suspended and do not coagulate. In case of adhesive collisions, the mass of the particle is an increasing function of time $m(t)$ and the height of the particle above the mid-plane $z(t)$ decreases. The vertical structure of the disk ρ_g is given by Eq. (1.3), assuming, as usual, a vertically isothermal disk in hydrostatic equilibrium.
If we let the particle in question settle toward the mid-plane according to the settling velocity Eq. (2.20), the equation of motion for the particle reads

$$\frac{dz}{dt} = u_{\text{settle}} = -\frac{3}{4\sigma}\frac{\Omega_K^2}{\rho_g \bar{u}}\, m(t)\, z(t),$$

which has to be solved coupled with the mass growth rate dm/dt. This quantity can be expressed as the amount of solid material in the volume swept out by the cross section σ_c of the particle collision with smaller dust grains:

$$\frac{dm}{dt} = \sigma_c \left| u_{\text{settle}} \right| f \rho_g(z) = \frac{3}{4}\frac{\Omega_K^2 f}{\bar{u}}\, m(t)\, z(t)$$

This two equations form a coupled set of ordinary differential equations. We have assumed for simplicity that $\sigma_c \sim \sigma$, since the evolving particle is much larger than the other suspended in the gas.
We show in Fig. (3.2), taken from Armitage (see [21]), numerical solutions for $z(t)/H_p$ and $a(t)$, with the initial conditions

$$\begin{cases} a(0) = 0.01\ \mu\text{m} \\ a(0) = 0.1\ \mu\text{m} \\ a(0) = 1\ \mu\text{m} \end{cases} \qquad \text{and} \quad z(0)/H_p = 5. \tag{3.11}$$

The adopted parameters are appropriate to a laminar disk at 1 AU, i.e. $H_p = 3 \times 10^{11}$ cm, surface density $\Sigma_g = 10^3\ \text{g cm}^{-1}$, $f = 0.01$, mean thermal speed $\bar{u} = 10^5\ \text{cm s}^{-1}$, solid density of the particle $\rho_s = 3\ \text{g cm}^{-3}$. Both particle growth and vertical settling are found to be extremely rapid: the grain grows exponentially as it sweeps up matter, reaching the mid-plane as a cm size pebble in a few hundred years. If we compare these time scales with the estimate of t_{settle} given in section (2.3), we immediately notice the enormous difference of more than two orders of magnitude, the parameters being slightly different but appropriate for the inner disk regions. It is also worth noticing

that the time taken to reach the mid-plane seems to be almost independent of the initial grain size.

We have hence described growth and sedimentation in a laminar disk, taking into account only the vertical differential settling relative velocity $\Delta u_{\rm settle}$ (which is equal to $u_{\rm settle}$ in our simple model), but we shall remind that a more complete description should consider also the other relative velocities sources.

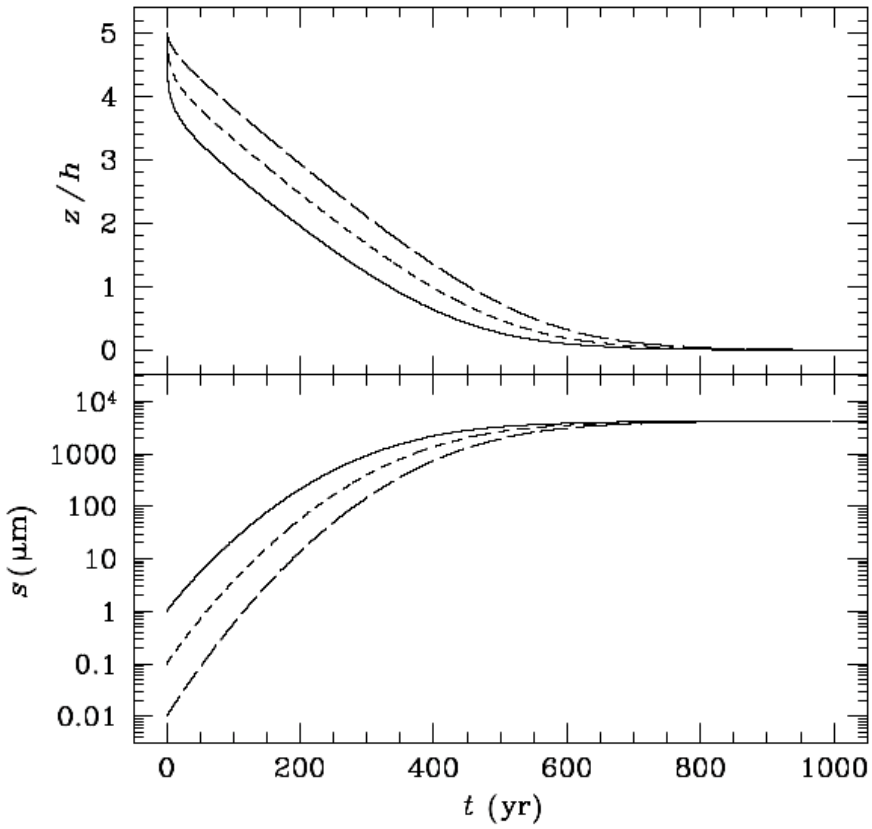

Figure 3.2: Numerical solutions for $z(t)/H_p$ and $a(t)$ for the growth and sedimentation model of a single particle settling toward the mid-plane, lifted from Armitage, 2010 [21]. The upper panel shows the height above the mid-plane as a function of time, the lower the particle radius $a(t)$. From top to bottom the curves are about $a(0) = 0.01\mu$m (long dashed line), $a(0) = 0.1\ \mu$m (dashed line) and $a(0) = 1\ \mu$m (solid line), all of them with an initial condition of $z(0)/H_p = 5$.

We shall ultimately consider the coagulative processes that may occur during the radial drift of a particle of radius a. The size dependence of the radial drift velocity (see Eq.(2.12)), in fact, introduces a relative velocity between particles of different radii, i.e. $\Delta u_{\rm RD}$, promoting collisions and (possibly) coagulation. As we did before, we can write the mass growth rate dm/dt for our particle as

the amount of solid material colliding adhesively with smaller grains as it drift inwards at the disk mid-plane:

$$\frac{dm}{dt} = \sigma_c \left| u_{r,d} \right| f \rho_g(0),$$

and we have assumed that the encountered smaller particles have already settled in the mid-plane. If we define now the growth time scale $t_{\rm growth}$ as follows

$$t_{\rm growth} \equiv m \left(\frac{dm}{dt} \right)^{-1},$$

we can easily make an estimate of the limits in which the effect of coagulative radial collisions affects the radial drift depletion of the solid surface density toward the central star imposing $t_{\rm growth} < t_{\rm drift}$, recalling the definition Eq. (2.21). If we make the reasonable assumption that a certain amount of vertical settling has already occured, we can make use of a higher dust-to-gas ratio $f = 0.1$, together with appropriate parameters in the inner disk (i.e. $\Sigma_g = 10^3\,\mathrm{g\,cm^{-3}}$, $\rho_s = 3\,\mathrm{g\,cm^{-3}}$ and $H_p/r = 0.05$), finding that

$$a \lesssim \frac{3f}{4\rho_s} \left(\frac{H_p}{r} \right)^{-1} \frac{\Sigma_g}{\sqrt{2\pi}} \simeq 1.9\,\mathrm{m},$$

which means that particles with a size up to $a \simeq 2$ m would collide with at least their own mass of other particles during their radial inward drift.
From this last estimates we can thus conclude that:

a) Grain growth due to the differential sedimentation happens on a very short time scale, much shorter than the typical lifetime of protoplanetary disks, and presents no problems for size scales from sub-micron up to cm;

b) Growth for radially drifting particles is likely to occur, provided that vertical settling has taken place, and can be due to very high relative velocities between actual rocks.

On the other hand we can always argue the survival of the population of very small grains (unquestionably observed in T-Tauri stars) to be incomprehensible, as well as the fact that very high relative velocities between large rocks will invalidate the simple hypothesis of hit-and-stick collisions. The phenomenon of fragmentation has hence to be considered in concert with these models, an analytically simple task (as we have seen in section(3.1)) but actually quite complicated in experimental limits.

* * *

Conclusions

The aim of this work was to analyse some of the most important physical processes regarding the evolution of the dust in a protoplanetary disk, the latter one described only marginally as the enviroment of the mechanisms of our interest. The evolution of the small material particles populating disks is complex yet essential for the study of the early stages of planets formation, an issue that concerns us very closely and from very long time.
We analysed some essential physics of a protoplanetary disk, then browsed the most important models of dust dynamics to conclude with a study of coagulative processes, starting from the now classic Smoluchowski equation (1916) while following some more recent theoretical patterns and keeping an eye on order of magnitude estimates where possible.

Through this brief overview we had also the chance to hint at some of the main problems of the past decades (and contemporary) studies, such as the origin of viscous stresses which allow the accretion, or the famous meter size barrier, because of which the growth from centimeter to meter size planetesimals remains a mystery; these are only the best known question marks though.

Hence the interest in the evolution of the protoplanetary disks' grains and in their mechanism of coagulation: tracing its roots back to a 18th century metaphysical and theological problem, even now this part of the protoplanetary disks' evolutive history is still a matter of interest, riding the wave of remarkable and decisive technology progress.

The author would like to sincerely thank Alessandro for the graphic support and the attentive, crucial help.

Bibliography

[1] Koerner, D. W., Sargent, A. I., and Beckwith, S. V. W., A rotating gaseous disk around the T Tauri star GM Aurigae, Icarus, **106** (Nov.), 2 (1993).

[2] Sargent, A. I., and Beckwith, S., Kinematics of the circumstellar gas of HL Tauri and R Monocerotis, ApJ **323** (Dec.), 294–305, (1987).

[3] McCaughrean, M. J., and O'Dell, C. R., Direct Imaging of Circumstellar Disks in the Orion Nebula. AJ, **111**, (1977).

[4] Kenyon, S. J., and Hartmann, L., Pre-Main-Sequence Evolution in the Taurus-Auriga Molecular Cloud, ApJS, **101**, 117 (1995).

[5] Evans, II, N. J., Dunham, M. M., Jørgensen, J. K., Enoch, M. L., Merìn, B., van Dishoeck, E. F., Alcalá, J. M., Myers, P. C., Stapelfeldt, K. R., Huard, T. L., Allen, L. E., Harvey, P. M., van Kempen, T., Blake, G. A., Koerner, D. W., Mundy, L. G., Padgett, D. L., and Sargent, A. I., The Spitzer c2d Legacy Results: Star-Formation Rates and Efficiencies; Evolution and Lifetimes, ApJS, **181** , 321–350 (2009).

[6] Williams, J. P., and Cieza, L. A., Protoplanetary Disks and Their Evolution (2011) ARAA, **49**, 67–117.

[7] Papaloizou, J. C. B., Pringle, J. E., Monthly Notices of the Royal Astronomical Society, **208**, 721 (1984).

[8] Bell, K. R., Cassen, P. M., Klahr, H. H., Henning, Th, Astrophysical Journal, **486**, 372 (1997).

[9] Lynden-Bell, D., Pringle, J. E., Monthly Notices of the Royal Astronomical Society, **168**, 603 (1974).

[10] Chapman, S. & Cowling, T. G., The Mathematical Theory of Non-uniform Gases, An Account of the Kinetic Theory of Viscosity, Thermal Conduction and Diffusion in Gases, 3rd edition, Cambridge University Press (1970).

[11] Eckhardt, B., Schneider, T.M., Hof, B., Westerweel, J., Turbulence Transition in Pipe Flow, Annual Review of Fluid Mechanics **39**, 447 (2007).

[12] Shakura, N. I., Sunyaev, R. A., Astronomy & Astrophysics, **24**, 337 (1973).

[13] Johansen, A., & Klahr, H., ApJ, **634**, 1353 (2005).

[14] Dzyurkevich, N. S., Flock, M., Turner, N. J., Klahr, H., & Henning, Th., Large Scale Azimuthal Structures Of Turbulence In Accretion Disks, Astrophysical Journal, **744** (2011).

[15] Pringle, J. E. & King, A. R., Astrophysical Flows, Cambridge University Press (2007).

[16] Hawley, J. F., Balbus, S. A., & Winters, W. F., Astrophysical Journal, **518**, 394 (1999).

[17] Whipple, F. L., From plasma to planet, p. 211, ed. A. Elvius, Wiley, London (1972).

[18] Weidenschilling, S. J., Monthly Notices of the Royal Astronomical Society, **180**, 57 (1977).

[19] Takeuchi, T. & Lin, D. N. C., Astrophysical Journal, **581**, 1344 (2002).

[20] Birnstiel, T., Dullemond, C. P., Brauer, F., Astronomy & Astrophysics **513**, A79 (2010).

[21] Armitage, P.J.: Astrophysics of Planet Formation (2010)

[22] Dubrulle, B., Morfill, G., & Sterzik, M., Icarus, **114**, 237 (1995).

[23] Fromang, S., & Papaloizou, J., A&A, **452**, 751 (2006).

[24] Smoluchowski, M. V., Zeitschrift fur Physik, **17**, 557 (1916).

[25] Dullemond, C. P., & Dominik, C., A&A, **434**, 971 (2005).

[26] Brauer, F., Dullemond, C. P., & Henning, T., A&A **480**, 859 (2008a).

[27] Blum, J., & Muench, M., Icarus, **106**, 151 (1993).

[28] Sirono, S. I., Icarus, **167**, 431 (2004).

[29] Dullemond, C. P., & Dominik, C. , A&A, **421**, 1075 (2004b).

[30] Safronov, V. S. 1969, Evolution of the protoplanetary cloud and formation of the earth and planets. English translation (1972)